Pergamon

Int. J. Heat Mass Transfer. Vol. 40, No. 10, pp. 2249–2259, 1997

0017–9310/97 $17.00+0.00

PII: S0017-9310(96)00310-9

Local characteristics of impingement heat transfer with oblique round free-surface jets of large Prandtl number liquid

C. F. MA, Q. ZHENG, H. SUN and K. WU

Department of Thermal Science and Engineering, Beijing Polytechnic University, Beijing 100022, China

T. GOMI

Department of Mechanical Engineering, Sophia University, Tokyo 102, Japan

and

B. W. WEBB

Department of Mechanical Engineering, Brigham Young University, Provo, UT 84602, U.S.A.

(*Received for publication* 9 *September* 1996)

Abstract—An experimental study was performed to investigate the local convective heat transfer from a vertical heated surface to an obliquely impinging circular free-surface jet of transformer oil. The effect of jet inclination was examined in the range of Reynolds number between 235 and 1745 with jet angle from 90 to 45 deg. Maximum heat transfer coefficient was found to decrease with the increasing of jet inclination, while its location shifted to the upstream side. Correlations were developed to predict the variations of the magnitude and the location of the peak heat transfer. Profiles of local Nusselt number were measured both in x and y-axes. The profiles along x-axis displayed an increasing asymmetry with increasing jet inclination. An empirical correlation was presented for predicting the x-axis profiles. With y-axis profiles, a symmetry appeared inside the stagnation zone, but a gravity-induced asymmetry was observed outside that zone.

1. INTRODUCTION

Impinging jets have been extensively employed in many industrial applications because of their excellent heat/mass transfer characteristics. In most cases air is used as the working fluid. The applications of gas jets include cooling of turbine blades and electronic components, tempering of glass, drying of textiles and paper, and annealing of metal and plastic sheets. Comprehensive surveys of gas jets have been presented by Martin [1], Downs and James [2] and Hrycak [3]. With liquid as cooling medium, the heat transfer coefficient can be increased several orders of magnitude in comparison with that of gas jets. Consequently, increased attention has been directed to the study of liquid jets recently [4–7]. Apparently, liquid jet impingement is a very promising candidate for the removal of high power densities encountered in many technical processes.

A significant amount of research on impingement heat transfer, both in analytical and experimental aspects, has been published. However, almost all the investigations are related to the condition in which the jets perpendicularly strike onto the solid surfaces. Oblique jets have only received relatively less attention. Most previous works on this topic dealt with the characteristics of flow fields of oblique axisymmetric air [8–14] or free-surface liquid [15, 16] jets both experimentally [8–12, 15, 16] and analytically [8, 13, 14]. Heat transfer with oblique air jets was first studied experimentally by Perry [17]. However, as commented by Sparrow and Lovell [18], his results can not be viewed with a high degree of reliability as he totally omitted the displacement of the point of maximum heat transfer from the point of the intersection of the geometrical axis of the jet and the impingement surface. This displacement was first measured by Sparrow and Lovell [18] using a mass transfer technique. They studied local mass transfer to an oblique impinging air jet at Reynolds number between 5000 and 10 000. Heat transfer to oblique round air jets was systematically studied by Goldstein and Franchett [19] at higher jet Reynolds number up to 35 000. Correlations of local heat transfer coefficient were presented. Moderate inclination-induced decreases in maximum coefficients were reported by both the two

NOMENCLATURE

A	area of heated surface, empirical constants
c	empirical constant
C_p	specific heat at constant pressure
d	jet nozzle diameter
h	local heat transfer coefficient
I	current intensity
k	thermal conductivity of fluid
m, n	empirical constants
Nu	hd/k, local Nusselt number
P	empirical constants
Pr	$C_p\mu/k$, Prandtl number
q	heat flux
R	electrical resistance
r	radial distance from stagnation point, recovery factor
Re	Ud/v, Reynolds number
s	displacement of the maximum heat transfer point from the geometric stagnation point
T_{aw}	adiabatic wall temperature
T_j	jet static temperature at nozzle exit
T_w	wall temperature
U	mean fluid velocity at nozzle exit
z	nozzle-to-plate spacing.

Greek symbols

θ	jet inclination angle
μ	dynamic viscosity
v	kinematic viscosity.

Subscripts

max	maximum value
o	normal impingement ($\theta = 0$).

investigations [18, 19]. More recently, local heat transfer with axisymmetric free-surface water jets was measured and correlated by Stevens and Webb [20] at Reynolds number from 6600 to 52 000. Significant differences were reported between free-surface liquid jets and submerged air jets, and attributed to the relative unimportance of entrainment and pre-impingement jet spreading for the free liquid jet. To the best knowledge of the present authors ref. [20] is the only one in open literature concerning heat transfer with circular free-surface oblique liquid jets. Reported in ref. [20] were the experimental results related to water jets ($Pr \approx 5$) impinging on horizontal targets. There may be significant differences for large Prandtl number liquid jets impinging on vertical surfaces, which are investigated experimentally in this work.

The purpose of the present paper is to characterize the local convective heat transfer from vertical heated surfaces to oblique free-surface jets of large Prandtl number at lower Reynolds number. All the main aspects of impingement heat transfer were examined in experimental detail. The present experiment was performed with single round free-surface transformer oil jets. The heated surface was maintained at constant heat flux condition. Local heat transfer coefficient was measured at jet velocity form 5.3 to 19.4 m s^{-1} with jet inclination ranging from 45 to 90 deg. The experimental results fill the gap of large Prandtl number oblique jets in the impingement heat transfer data base. In practise, investigations of liquid jet impingement have been stimulated and promoted by electronic cooling [21–24]. Besides electronic devices, the results of this study can find their applications in oil-cooled engines [25] in which oblique oil jets have been used for cooling of hot spots on pistons or cylinder heads.

2. EXPERIMENTAL APPARATUS AND METHOD

Transformer oil was chosen as the test liquid in this study. The test liquid was circulated in a closed loop which had provision for filtering, metering, preheating and cooling. The test chamber was constructed of stainless steel with three visual ports as illustrated in Fig. 1. The bottom section of the cover on the chamber was transparent. A flexible polyethylene tube joined the two sections of the cover. The test section assembly was vertically fixed on one side of the chamber. The details of the test section are presented in Fig. 2. The main part was a strip of 10 μm thick constantan foil with a heated section of 10 × 5 mm (nominal) exposed to the coolant. The strip on either side of this active section was soldered to copper busbars, which were in turn connected to power leads. The heated section of the foil was cemented to a bakelite block inserted between the copper busbars. The assembly was cemented in a Plexiglas disk fixed in a brass housing with a screwed flange. The test section was highly insulated thermally by fibreglass to minimize heat loss. The temperature of the centre of the inner surface of the heater was measured with a 40 gage iron-constantan thermocouple which was electrically insulated from the heater yet in close thermal contact. The active section of the constantan foil was used as an electrical heating element as well as a heat transfer surface. AC power to the test section was provided by a 50 A power supply. The intensity of the current through the test section was measured by an ammeter.

An oil jet was issued from a horizontal jet tube of 0.987 mm inside diameter and 35 mm length. The large length-to-diameter ration ensured the full development of laminar pipe flow at the nozzle exit. As

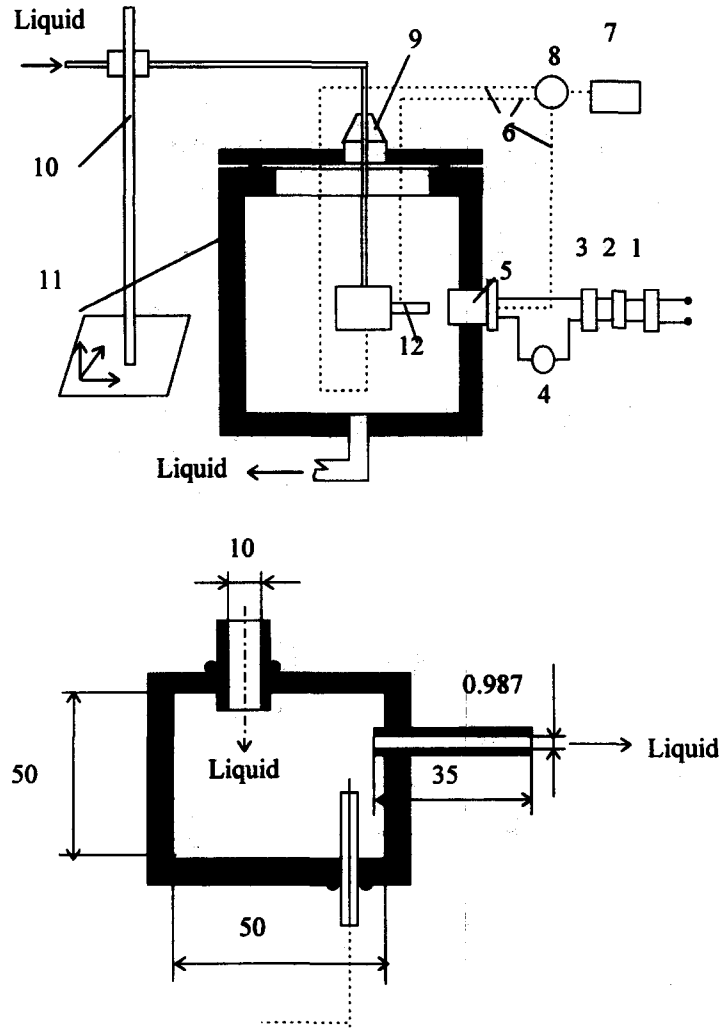

Fig. 1. Details of test chamber and instrumentation (all dimensions in mm). (1) Stabilized voltage supply; (2) voltage regulator; (3) voltage transformer; (4) amperemeter; (5) test section assembly; (6) thermocouples; (7) MV meter; (8) switcher; (9) flexible plastics; (10) three-dimensional coordinate frame; (11) chamber; (12) jet tube.

shown in Fig. 3(a) the oil was supplied from a vertical delivery tube (a) to the jet nozzle (b) passing a plenum box (c). Both the jet tube and the delivery tube were made of stainless steel and fixed with the plenum box. Their axes were perpendicular with each other in a vertical plane. The jet tube could be rotated in the horizontal plane about the axis of the delivery tube by pivoting the latter upon a pivot bearing (d). The inclination of the jet tube to the test section could be read by the angle markings scribed on the surface of a horizontal plate (e) with an estimated angular uncertainty of ± 1 deg. The jet tube-delivery tube assembly was fixed on a three-dimensional coordinate rack and could be adjusted with respect to the test section (f) with placements accomplished within ± 0.01 mm. The jet temperature was measured with a 40 gage iron-constantan thermocouple placed inside the plenum box close to the entrance of the jet tube. The oil temperature in the test chamber was also monitored by a thermocouple of the same type. Due to the flexible nature of the plastic seal at the top of the chamber, the pressure in the chamber is considered close to the atmosphere.

The heat transfer surface was left in the original highly polished condition and cleaned with acetone before tests. Heat flux was calculated from the electrical power supplied to the test section and the area of one side of the heated surface. Heat flux was determined by the following formula:

$$q = I^2 R/A \tag{1}$$

where the resistance R was measured accurately with direct current before experiments. It was verified in preliminary tests that the variation of resistance with temperature could be neglected (less than $\pm 0.1\%$), as the heater temperature variation was less than 40 K in the present study and the variation in resistivity with temperature is extremely small for constantan. The area A of the heated surface was carefully mea-

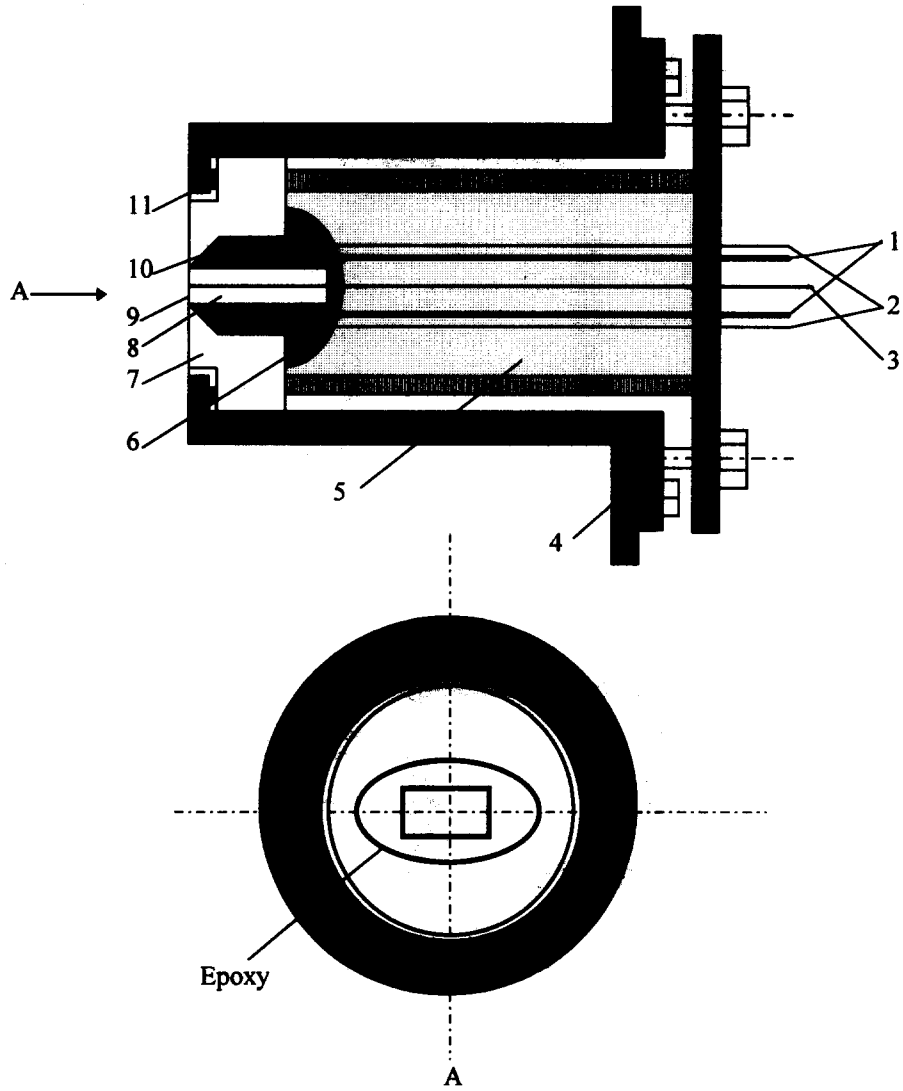

Fig. 2. Details of electrically heated test section. (1) Power lead; (2) voltage tap; (3) thermocouple; (4) tank wall; (5) fiberglass; (6) epoxy; (7) plexiglass; (8) bakelite; (9) 10 μm thick constantan foil; (10) copper block; (11) O-ring.

sured for each test section assembly with a tool makers microscope of 0.001 mm resolution.

In preliminary experiments the jet tube was oriented normal to the test section. The distance between the nozzle and the target surface was accurately adjusted by means of the three-dimensional frame. In order to ensure that the nozzle centerline coincided with the midpoint of the heater, a procedure of centering was developed whereby the normally impinging jet was moved on the heated surface until the minimum wall temperature was recorded by the thermocouple. In experiments with oblique jets, the jet inclination angle was fixed and the jet tube was adjusted again by the three-dimensional rack to warrant the coincidence of the center of the heater with the geometric intersection of the jet axis and the impingement plane at a fixed nozzle-to-plate spacing. The measured wall temperature at the heater center was taken as the local value. By recording this temperature for various locations of the jet tube, both horizontal (x-axis) and vertical (y-axis) temperature distributions could be obtained for given jet conditions and surface heat fluxes. Properties of the working fluid were evaluated at the film temperature by averaging the wall and jet temperature. The local heat transfer coefficient was calculated from the heat flux and the local wall temperature:

$$h = \frac{q}{T_w - T_{aw}} \tag{2}$$

where the adiabatic wall temperature T_{aw} was determined by

$$T_{aw} = T_j + r\frac{U^2}{2C_p} \tag{3}$$

where the velocity U was calculated from the measured flow rate and the nozzle area. Great significance

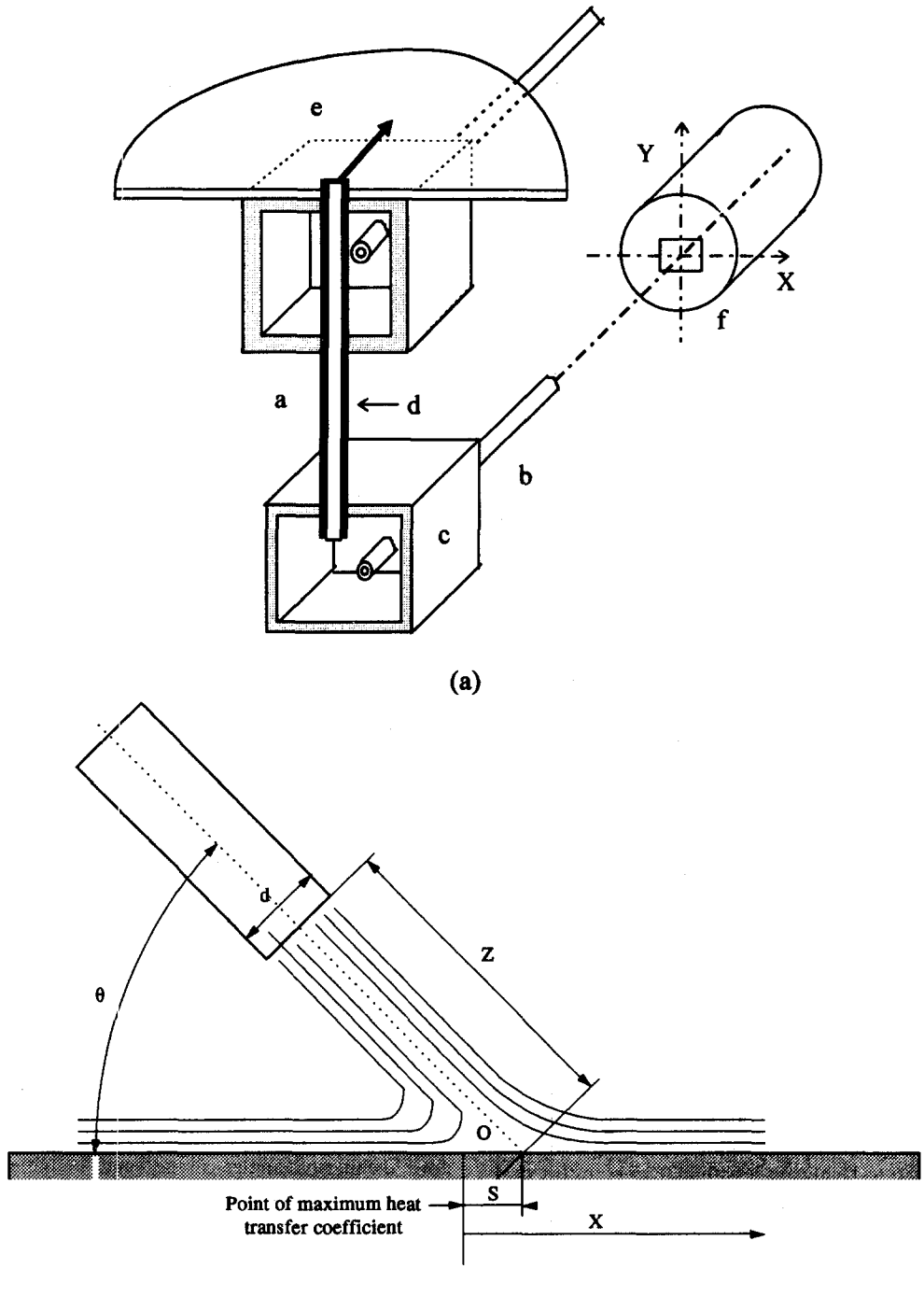

Fig. 3. Details of nozzle assembly (a) and coordinate assembly (b).

of recovery effect has been verified both experimentally [26–28] and numerically [29, 30] for perpendicular impinging jets of large Prandtl number liquid. Detailed information of recovery factors has been reported. For oblique jets of transformer oil radial distribution of recovery factors were measured at various inclination angles in this work. The result is presented in Fig. 4.

During the experiment, the difference between T_w and T_{aw} was adjusted to be maintained approximately at 10 K. The uncertainty in Nusselt number was influenced primarily by the determination of heat flux and wall temperature. The surface heat flux was affected by the variation of the constantan foil thickness that was claimed in the suppliers specification to be less than $\pm 3\%$ of the normal value. This value is taken as the indicator of heat flux variation due to foil thickness nonuniformity. Preliminary experiments were per-

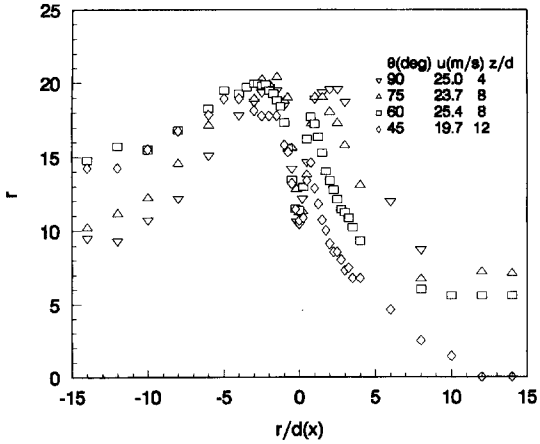

Fig. 4. Radial distributions of measured recovery factors.

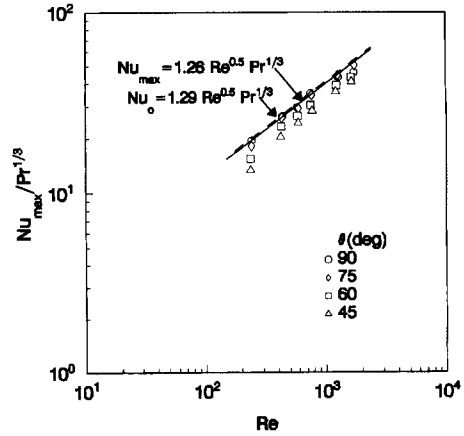

Fig. 5. Variation of maximum Nusselt number.

formed to check heat loss from the heater, and indicated that with jet impingement the maximum conduction loss to the back of the heater assembly was less than 0.8% of the power input to the heater. This conclusion was supported by a conduction analysis for this study. Therefore, no correction was included for such conduction loss in this work. The determination of the heater surface temperature was related to the thermal resistance of the adhesive layer between the thermocouple bead and the back side of the foil. During the manufacture process the foil was firmly pressed to the top surface of the bakelite block to minimize the thickness of the adhesive layer in between. Measurements were made of the adhesive thickness with several used test sections after their failure in experiments. The thickness was determined to be between 0.04 and 0.1 mm. Taking the typical value of the thermal conductivity of adhesive as 0.29 W $m^{-1} \cdot K^{-1}$, the thermal resistance across the adhesive layer was estimated between 1.4×10^{-4} and 3.4×10^{-14} $m^2 \cdot K\ W^{-1}$. As the conduction heat loss was less than 0.8% of the power input, and its main part passed through the bus bars, the uncertainty arising from positioning of the thermocouple bead was estimated to be always less than 0.15 K in this study. Another source of the uncertainty in wall temperature was concerned with lateral heat conduction along the constantan foil caused by the sharp radial variation of the heat transfer coefficient around the stagnation zone. Using the measured wall temperature distribution, this uncertainty was determined to be negligible (less than 0.8%) due to the extremely small thickness of the foil. All the thermocouples were calibrated to an accuracy of ± 0.1 K before experiments. The uncertainty in Nusselt number was determined to be less than $\pm 5\%$. The uncertainty in Reynolds number was affected by the measurement of the flowrate and the nozzle exit area. While the flowmeter was carefully calibrated, the nozzle exit area was precisely determined using the tool maker's microscope of 0.001 mm resolution. The uncertainty in Reynolds number did not exceed $\pm 5.5\%$.

3. EXPERIMENTAL RESULTS AND DISCUSSION

3.1. *Variation of maximum heat transfer coefficient*

Variation of maximum heat transfer with jet inclination has been studied experimentally with submerged air jets [18, 19]. A clear trend was found in the two investigations that the maximum transfer coefficients decreased with increasing inclination. Over the range of angles from 90 to 30 deg, the decrease was reported as large as 15–20% for $Re = 2500$–$10\,000$ [18] or 20–30% for $Re = 10\,000$–$35\,000$ [19]. Free-surface liquid jet experimental data have been presented by Stevens and Webb [20] with water as working fluid. Because of the large scatter of their data, it seems difficult to determine a clear trend of the variation from the measurements reported in ref. [20]. As ref. [20] probably is the only report on local heat transfer with oblique liquid jets in the open literature, the problem seems to remain unsolved for impinging liquid jets. It is noted that all the previous investigations [18–20] did not present any quantitative correlation to predict the variation of maximum heat transfer with Reynolds number and jet inclination. In the present investigation the variation of maximum heat transfer magnitude was carefully measured at four inclination angles in the range of jet velocity between 3.3 and 23.8 m s^{-1}. The experimental data are presented in Fig. 5. An empirical correlation for the maximum heat transfer at different inclination angle was developed of the following form

$$Nu_{\max} = CPr^n Re^m \tag{4}$$

where the exponent n of Prandtl number was set to 1/3 according to the result of ref. [26]. for viscous oil. The Reynolds number power m and the coefficient C were determined from the least-squares fit for different inclinations. Their values are given in Table 1. The exponent m was determined to be 0.5, which is entirely identical with those obtained in refs. [4, 20, 22, 26]. In Fig. 5 the correlation proposed by Ma *et al.* [26] for normal impingement is also presented for comparison. The two correlations are almost identical.

With the constants in Table 1, eqn (4) fits 96% of

Table 1. Correlation coefficients in eqn (4)

θ [deg]	90	75	60	45
C	1.26	1.22	1.09	0.986
m		0.5		
n		1/3		

the data within $\pm 10\%$ for all measured Reynolds numbers and jet angles. Good agreement can be seen in Fig. 5 between the experimental data and the predicted curve for perpendicular impingement. Over a small range of incidence angles ($\theta = 90$–75 deg), the effect of incidence angle on peak heat transfer is very slight—less than 5%. With the angle between 75 and 45 deg, moderate decreases were observed. At a jet angle of 45 deg the average reduction of maximum heat transfer coefficient is about 22% in comparison with that for normal impingement. This decrease is quite close to the results for air jets [18, 19]. It is also found that the decrease in maximum heat transfer with the increasing inclination is only slightly influenced by Reynolds number in the range of the present study. It is interesting to note that all the above trends observed in the present investigation are consistent with those reported by previous studies [18, 19] although the working conditions, including type of jets, configuration of nozzles, working fluids, Reynolds number and Prandtl number, are quite different from each other.

3.2. *Displacement of maximum heat transfer position*

Besides its magnitude, the location of maximum heat transfer is also significantly influenced by jet inclination as shown in Fig. 3(b). It was reported by Stevens and Webb [20] that the upstream displacement of maximum heat transfer point from the geometric intersection of jet axis with the impingement plane for free-surface water jets was significantly less than that measured with submerged jets [18, 19]. No quantitative correlation for the shift was presented in previous work [18–20] both for circular air and water jets. In the present study, the displacement was accurately measured with oblique oil jets issuing from a tube of 3 mm (nominal) diameter. A correlation is developed and presented. The measured displacements normalized by the jet diameter d are plotted in Fig. 6 as a function of the inclination angle θ. The measurement were made at four Reynolds numbers with jet velocity ranging from 1.84 to 3.74 m s^{-1}. As shown in Fig. 6 the displacement increases monotonically with the increasing of inclination. Moderate scatter in the data is seen from Fig. 6. In the range of Reynolds number studied here, the effect of Reynolds number on displacement seems very weak. All the data can be well correlated by the following equation:

$$s/d = (0.119 + 0.00454\theta)\cos\theta \qquad (5)$$

where the jet angle θ is expressed in radians. As shown

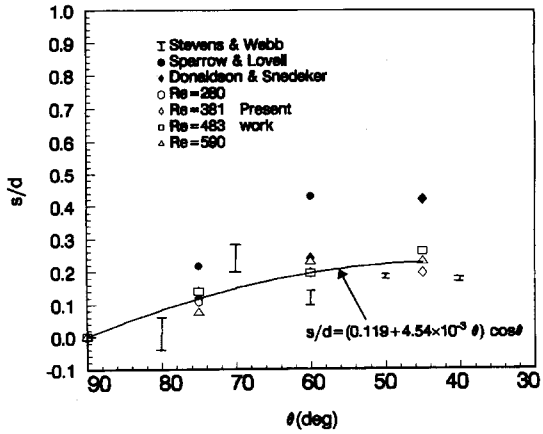

Fig. 6. Effect of jet inclination on the displacement of the maximum heat transfer point.

in Fig. 6 the predicted curve by eqn (5) generally agrees with all the measured results from the present work. In Fig. 6 the data reported in ref. [20] for water jets are also presented for comparison. Their data showed significantly more scatter than those in the present work. However, the two results demonstrate approximate magnitude of the displacement. The data of Sparrow and Lovell [18] for submerged air jets are given in the figure. Their observed displacements are remarkably higher than those with liquid free-surface jets. The difference can be attributed to the stronger entrainment and consequent pre-impingement spreading for submerged jets.

In some previous investigations of pure fluid mechanics study for impinging air jets, static pressure on the impingement surface was measured and upstream displacement of the maximum pressure point from the geometric impingement point was recorded [8–12]. Although it has been pointed out [18] that the maximum pressure point may not coincide with the maximum heat transfer point, it is worth comparing the fluid mechanic results with those of heat transfer. The measured displacements of maximum pressure point reported by Donaldson and Snedeker [9] are presented in Fig. 6. It is noted that the displacement of maximum pressure is in agreement with the data of present work in the case of small inclination ($\theta = 90$–60 deg), but for larger inclination the measured displacement of maximum pressure is significantly higher than the present result. It should be emphasized that all the comparative data were taken at working conditions very different from the present work.

3.3. *Local distribution of heat transfer coefficient*

Local measurements were made at four incidence angles (90, 75, 60, 45 deg) of heat transfer coefficients along the two principal axes of the wall jets (x- and y-axes) with the Reynolds number ranging from 210 to 1033. The nozzle-to-plate spacing was fixed at 4 jet-orifice diameters. In order to examine the effect of Reynolds number, the distributions along x- and y-axes were measured at five and two Reynolds

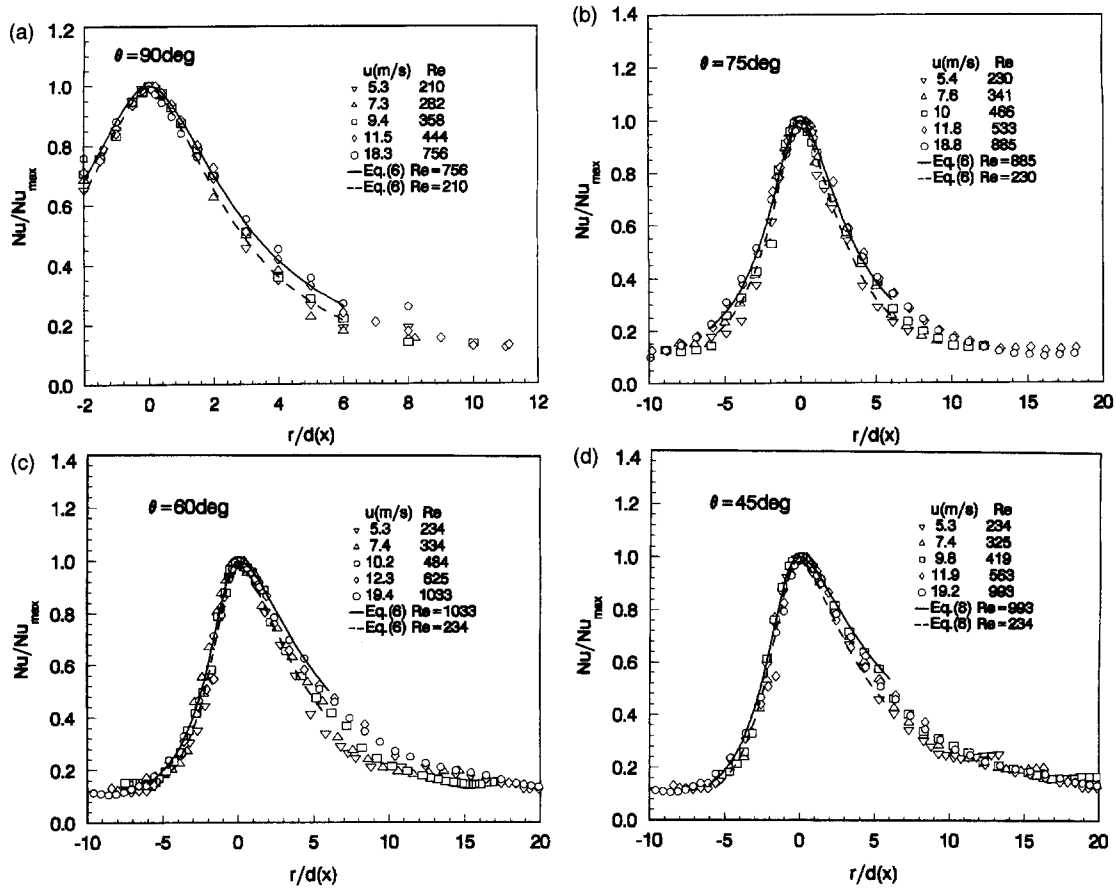

Fig. 7. Normalized local Nusselt number profiles along x-axis: (a) $\theta = 90$ deg; (b) $\theta = 75$ deg; (c) $\theta = 60$ deg; (d) $\theta = 45$ deg.

numbers, respectively. After normalization by the maximum heat transfer coefficient the distributions of the local Nusselt number along the x-and y-axes are presented in Figs. 7 and 8, respectively. As shown in Fig. 3(b), the origin situated at the point of maximum heat transfer points along the x-axes. In general, the distribution curves are characteristic of bell shape as reported by many previous investigators.

3.3.1. *Nusselt number profiles along x-axis.* Figure 7(a) demonstrates the plots of local Nusselt number profiles of perpendicular impingement. It is seen from the figure that the distribution curves are symmetric about the stagnation point. The asymmetry in the profiles may be quantified as a difference in the Nusselt number values at corresponding radial positions on either side of the stagnation point divided by the average of the two values. The asymmetry for all the normal impingement data was found to be less than 5% in the stagnation zone ($r/d < 2$). With oblique impingement an increasing asymmetry is observed in the Nusselt number profiles as the jet inclination increases [Fig. 7(b–d)]. It is clearly evident from Fig. 7 that with increasing jet incidence angles the heat transfer rate on the upstream direction side drops off more rapidly while that on downstream tends to decline more slowly. The heat transfer rate on the side downstream of the maximum heat transfer point is higher than that on the upstream. The difference between the two heat transfer rates tends to increase with increasing the jet inclination. This asymmetry can be explained by the fact that the flow rate towards the downstream direction is higher than that upstream because of the initial inertia of the impinging oblique jet flow. The dependence of local heat transfer on Reynolds number may be examined more clearly with the distribution data normalized to the maximum heat transfer rates as shown in Fig. 7. Local Nusselt numbers are found to be only very slightly dependent on Reynolds number after the normalization in the present work. The figures indicate that the local heat transfer is essentially independent of the Reynolds number inside the stagnation zone. Beyond this region a weak dependence is observed. It seems that the distribution curves drop off a little bit more slowly as the Reynolds number increases.

An attempt was made to develop a correlation of local Nusselt number distribution along x-axis. All the local heat transfer data in the range of $|r/d| < 6$ can be well correlated by

$$\frac{Nu}{Nu_{\max}} = \frac{K(Re)^{q|r/d|}}{1 + A|r/d|^{p}} \tag{6}$$

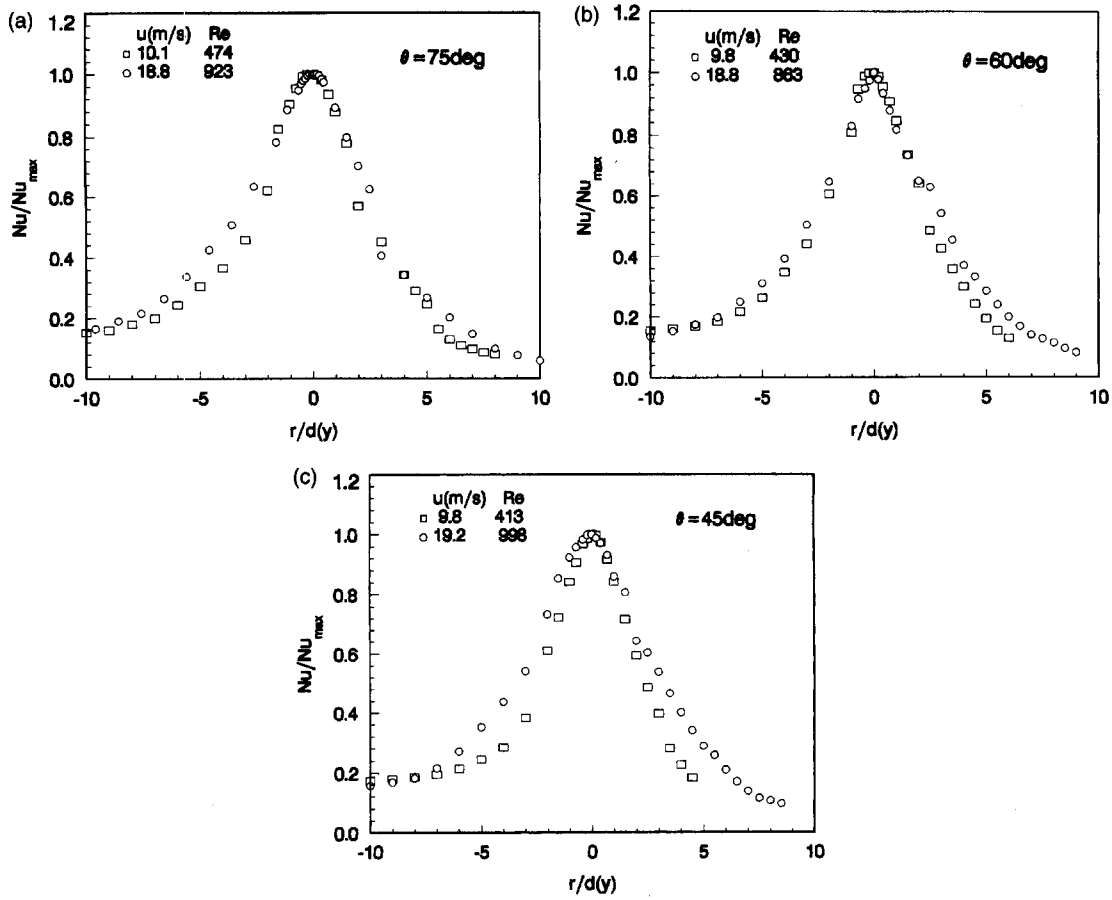

Fig. 8. Normalized local Nusselt number profiles along y-axis: (a) $\theta = 75$ deg; (b) $\theta = 60$ deg; (c) $\theta = 45$ deg.

where,

$$A = A_0 + A_1 \sin\theta + A_2 \sin^2\theta \tag{7a}$$

$$P = P_0 + P_1\theta + P_2\theta^2. \tag{7b}$$

The correlation coefficients K, q, A_0, A_1, A_2 and P_0, P_1, P_2 in eqns (6) and (7) were obtained by a least-squares technique. These values are given in Table 2. It is noted that the insignificant influence of Reynolds number has been taken into account in eqn (7) with the weak function of Reynolds number $Re^{0.0274|r/d|}$. Nu_{max} can be calculated from eqn (4). Equation (6) fits 90% of the data within $\pm 8\%$ for all the measured Reynolds numbers and jet angles. The predicted curves by eqn (6) are presented in Fig. 7 for comparison with the experimental data. Good agreement is seen between the correlation curves and the corresponding data at different working conditions.

3.3.2. *Nusselt number profiles along y-axis.* Local heat transfer coefficient along y-axis was measured at $\theta = 75$, 60 and 45 deg. The results are plotted in Fig. 8 after normalization to maximum Nusselt number. If comparisons are made from figure to figure among Fig. 8(a–c), it can be seen that by contrast to the x-axis profiles the local heat transfer coefficient distributions along the y-axis seem to be insensitive to jet inclination in the ranges of the parameter encountered in this study. This trend was also reported with oblique air jets in ref. [18]. As shown in Fig. 8, good symmetry of y-axis profiles about x-axis is expectantly observed in

Table 2. Empirical constants in eqns (6) and (7)

Coefficient	A_0	A_1	A_2	P_0	P_1	P_2	K	q
$r/d > 0$	1.38	−3.31	2.07	0.643	1.51	−0.522	0.00218	0.0274
$r/d < 0$	−1.58	4.02	−2.29	3.92	−2.70	0.835	0.00218	0.0274

the stagnation zone. This result is consistent with the air jet reports [18, 19]. However, in contrast to the air jet results asymmetry in the y-axis profiles is found beyond the stagnation zone. Figure 8 indicates that the local Nusselt number on the vertical heat transfer surface decays more rapidly along the y-axis above the maximum heat transfer point (origin of the x-y system) than below it. This asymmetry may be attributed to the influence of gravity on the flow at low Reynolds number. Gravity force assists the down-flow of wall jets enhancing the local heat transfer below the impingement point, while it opposes the up-flow resulting in the deterioration of the heat transfer above the point.

The effect of Reynolds number of the y-axis profiles can be examined with the normalized curves in Fig. 8. It is found that the normalized profiles are almost independent of Reynolds number in the stagnation zone. In the wall jet zone ($r/d > 2$), a very slight dependence on Reynolds number is observed.

4. CONCLUSIONS

Measurements were made to investigate the local characteristics of convective heat transfer from a vertical heated surface to oblique circular free-surface jets of transformer oil in the range of jet Reynolds number between 235 and 1745. The effect of jet inclination was studied in experimental detail. Based on the data, the following conclusions may be drawn:

(1) The maximum local Nusselt number was determined to diminish with the increasing of jet inclination. The variation of maximum Nusselt number with Reynolds number at various jet angles can be correlated by eqn (4).

(2) Displacement of the maximum heat transfer point from the geometric stagnation point was measured at various Reynolds numbers. A correlation (eqn (5)) was developed to predict the variation of the displacement with jet angles. The magnitude of the shifts with free-surface oil jets was found to be significantly less than that with oblique submerged jets.

(3) X-axis profiles of local Nusselt number exhibited an increasing asymmetry about the maximum heat transfer point with the increasing of jet inclination. The x-axis profiles can be well correlated by eqn (6).

(4) Y-axis profiles of local Nusselt numbers were found to be insensitive both to jet angle and Reynolds number. However, the influence of gravity was observed resulting in asymmetry in wall jet zone.

Acknowledgment—This work was supported by the National Natural Science Foundation of China. The authors are indebted to Mr D. H. Lei and Ms C. J. Feng for their assistance in the experiments, and to Professor S. Y. Ko for his valuable suggestions.

REFERENCES

1. Martin, H., Heat and mass transfer between impinging gas jets and solid surfaces. *Advances in Heat Transfer*, 1977, **13,** 1–60.
2. Downs, H. T. and James, E. H., Jet impingement heat transfer—A literature survey. *ASME Paper*, 1987, 87-HT-35.
3. Hrycak, P., Heat transfer from impinging jets—A literature review. Technical Report AFWAL-TR-81-3504, Flight Dynamics Laboratory, Wright Patterson AFB, OH, 1981.
4. Faggiani, S. and Grassi, W., Impingement liquid jets on heated surface. In *Proceedings of the 9th International Heat Transfer Conference*, Vol. 1, 1990, pp. 275–285.
5. Ma, C. F., Liquid jet impingement heat transfer with or without boiling. In *Proceedings of the 10th National Heat Transfer Congress*, Genova, Italy, June 25–27, 1992, pp. 35–60.
6. Womac, D. J., Ramadhyani, S. and Incropera, F. P., Correlating equations for impingement cooling of small heat surfaces with single circular liquid jets. *ASME Journal of Heat Transfer*, 1993, **115,** 106–115.
7. Webb, B. W. and Ma, C.-F., Single phase liquid jet impingement heat transfer. *Advances in Heat Transfer*, 1995, **26,** 105–217.
8. Beltaos, S., Oblique impingement of circular turbulent jets. *Journal of Hydraulic Research*, 1976, **14,** 17–36.
9. Donaldson, C. S. and Snedeker, R. S., A study of free jet impingement, Part 1, mean properties of free and impinging jets. *Journal of Fluid Mechanics*, 1971, **45,** 281–319.
10. Foss, J. F. and Kleis, S. J., Mean flow characteristics for the oblique impingement of an axisymmetric jet. *AIAA Journal*, 1976, **14,** 705–706.
11. Foss, J. F., Measurements in a large-angle oblique jet impingement flow. *AIAA Journal*, 1979, **17,** 801–802.
12. Lamon, P. J. and Hunt, B. L., The impingement of underexpanded, axisymmetric jets on perpendicular and inclined flat plates. *Journal of Fluid Mechanics*, 1980, **100,** 471–511.
13. Rubel, A., Computations of the oblique impingement of round jets upon a plane wall. *AIAA Journal*, 1981, **19,** 863–871.
14. Rubel, A., Oblique impingement of a round jet on a plane surface. *AIAA Journal*, 1982, **20,** 1756–1758.
15. Taylor, G., Formation of thin flat sheets of wall. *Proceedings of The Royal Society A*, 1960, **259,** 1–17.
16. Schach, W., The deflection of a free liquid jet on a flat plane. *Ingenieur-Archiv*, 1934, **5,** 245–265.
17. Perry, K. P., Heat transfer by convection from a hot gas jet to a plane surface. *Proceedings of the Institute of Mechanical Engineers*, 1954, **168,** 775–780.
18. Sparrow, E. and Lovell, B. J., Heat transfer characteristics of an obliquely impinging circular jet. *ASME Journal of Heat Transfer*, 1980, **102,** 202–207.
19. Goldstein, R. J. and Franchett, M. E., Heat transfer from a flat surface to an oblique impinging jet. *ASME Journal of Heat Transfer*, 1988, **110,** 84–90.
20. Stevens, J. and Webb, B. W., The effect of inclination on local heat transfer under an axisymmetric free-liquid jet. *International Journal of Heat and Mass Transfer*, 1991, **34,** 1227–1236.
21. Ma, C. F. and Bergles, A. E., Boiling jet impingement cooling of simulated microelectronic chips. *ASME HTD*, 1983, **28,** 5–12.
22. Sun, H., Ma, C. F. and Nakayama, W., Local characteristics of convective heat transfer from simulated microelectronic chips to impinging submerged round water jets. *ASME Journal of Electronic Packaging*, 1993, **115,** 71–77.
23. Jiji, L. M. and Dagan, Z., Experimental investigation of single phase multi-jet impingement cooling of an array of microelectronic heat sources. *Cooling Technology for*

Electronic Equipment, Ed. Win Aung. Hemisphere, New York, 1988, pp. 333–352.
24. Wadsworth, D. C. and Mudawar, I., Cooling of multichip electronic module by means of confined two-dimensional jets of dielectric liquid. *ASME Journal of Heat Transfer*, 1990, **112,** 891–898.
25. Kiryu, M., Development of oil-cooled 750 cc motorcycle engine. *Automobile Technology*, 1986, **40,** 1154–1158 (in Japanese).
26. Ma, C. F., Sun, H., Auracher, H. and Gomi, T., Local convective heat transfer from vertical heated surfaces to impinging circular jets of large Prandtl number liquid. *Proceedings of the 9th International Heat Transfer Conference*, 1990, **2,** 441–446.
27. Ma, C. F., Zheng, Q., Lee, X. C. and Gomi, T., Impingement heat transfer and recovery effect with submerged jets of large Prandtl number liquid—I. Unconfined circular jets. *International Journal of Heat and Mass Transfer*, 1996, **40,** 1481–1490.
28. Lee, X. C., Ma, C. F., Zhuang, Y. and Zheng, Q., Experimental research on recovery effect of liquid circular jet impingement. *Proceedings of the 3rd International Symposium on Multiphase Flow and Heat Transfer*, Xian, China, 1994, pp. 456–463.
29. Lee, X. C., Ma, C. F., Zheng, Q., Zhuang, Y. and Tian, Y. Q., Numerical study of recovery effect and impingement heat transfer with submerged circular jets of large Prandtl number liquid. *International Journal of Heat and Mass Transfer*, 1997, in press.
30. Li, D. Y., Guo, Z. Y. and Ma, C. R., Relationship between recovery factor and viscous dissipation in a confined impinging circular jet of high Prandtl number liquid. *International Journal of Heat and Fluid Flow* (submitted).